

# On Joint Frequency and Power Allocation in a Cross-Layer Protocol for Underwater Acoustic Networks

Josep Miquel Jornet, *Student Member, IEEE*, Milica Stojanovic, *Fellow, IEEE*, and Michele Zorzi, *Fellow, IEEE*

**Abstract**—Path loss in an underwater acoustic channel depends not only on the transmission distance, but also on the signal frequency. As a result, the useful bandwidth decreases with distance, a feature not normally present in terrestrial radio networks. This fact motivates the use of multihop communications in an acoustic network, and strongly influences its design, since the same set of protocols will exhibit different performance when operating in a different frequency range. Multihop transmission is considered for large area coverage in acoustic networks, with an eye towards efficient power and bandwidth allocation. Power control is used as a practical means of optimizing the overall performance across the physical, medium access control (MAC) and routing layers. A geographic routing technique, called the focused beam routing (FBR), which requires each node to know only its own location and that of the final destination, is coupled with the distance aware collision avoidance protocol, which regulates the channel access. Results show that the average energy per bit consumption is reduced by adjusting the power, center frequency, and bandwidth in accordance with the network node density. Specifically, as the density increases, greater bandwidths offer per-hop energy reduction as well as a reduced packet collision rate.

**Index Terms**—Cross-layer design, energy efficiency, frequency allocation, medium access control (MAC), power control, routing, underwater acoustic networks.

## I. INTRODUCTION

UNDERWATER wireless communications have witnessed major developments in the last decade. While the initial applications involved just a single transmitter and a receiver

Manuscript received August 19, 2009; accepted September 08, 2010. This work was supported by the National Science Foundation (NSF) under Grants 0520075 and 0831728, the National Oceanic and Atmospheric Administration (NOAA) under Sea Grant NA060AR4170019, and the Italian Institute of Technology under the “ProjectSeed” program. Part of this work was presented at the ACM Third International Workshop on Underwater Networks (WuWNet), San Francisco, CA, September 2008 and the IEEE Oceans Conference, Quebec City, QC, Canada, September 2008.

**Associate Editor:** C. de Moustier.

J. M. Jornet was with the MIT Sea Grant College Program, Massachusetts Institute of Technology, Cambridge, MA 02139 USA. He is now with the Broadband Wireless Networking Laboratory, School of Electrical and Computer Engineering, Georgia Institute of Technology, Atlanta, GA 30332 USA (e-mail: jmjornet@ece.gatech.edu).

M. Stojanovic is with the Department of Electrical and Computer Engineering, Northeastern University, Boston, MA 02115 USA (e-mail: millitsa@ece.neu.edu).

M. Zorzi is with the Department of Information Engineering (DEI), University of Padova, Padova 35122, Italy (e-mail: zorzi@dei.unipd.it).

Color versions of one or more of the figures in this paper are available online at <http://ieeexplore.ieee.org>.

Digital Object Identifier 10.1109/JOE.2010.2080410

communicating at low bit rates, underwater communications today are associated with complex systems requiring networking of multiple devices [1]–[3]. These novel applications range from autonomous observation systems to cooperative missions between autonomous underwater vehicles (AUVs), bottom-mounted nodes, and surface crafts.

The main challenges in underwater communications are posed by the high-attenuation and bandwidth-limited underwater acoustic channel. Despite the advances in underwater wireless electromagnetic communications, their use is limited to a very short range, and can thus be seen as a complementary technique for very specific applications [4]. Acoustic technology is the chosen physical layer for almost all applications in which a coverage greater than a few hundred meters is required. This has its own shortcomings, such as multipath fading or Doppler shift and spread, and motivates the use of advanced modulation techniques and sophisticated transceiver architectures.

One of the unique properties of the underwater acoustic channel is that the total signal attenuation depends not only on the distance, but also on the signal frequency [5]. As a result, the available bandwidth increases as the distance shortens. This phenomenon encourages the use of relay networks and the development of multihop solutions. Multihopping is a well-established transmission technique in radio communication systems, in which battery-powered nodes should minimize their energy consumption without compromising the network connectivity and the ability to deliver data to a final destination. Reducing the average transmission distance by including several intermediate nodes within the path to the destination allows nodes to limit their transmission power. When it comes to the underwater channel, multihop communication offers not only the benefits of power reduction, but also the possibility to utilize a greater bandwidth.

Multihopping introduces new challenges to the communication system design, spanning all layers of the network architecture. First and foremost, power control at the physical layer dictates resource utilization as well as the network topology. Taking into account the random nature of *ad hoc* networks, in which both voluntary and involuntary motions take place, variable transmission power should be considered. In turn, the ability to control power alters the performance of the existing medium access control (MAC) protocols and enables new routing mechanisms, thus motivating the development of integrated solutions.

In this paper, a cross-layer design for underwater acoustic networks is proposed and evaluated under different power and frequency allocation schemes with focus on minimum energy consumption. The routing protocol, the MAC, and the physical layer functionalities are tightly coupled through a judicious allocation of power and bandwidth. The routing protocol decides which power level should be used in light of different criteria, and by different mechanisms. The MAC then adapts specific parameters, such as waiting or backoff times, according to the new transmission distance. Switching the transmission power to a new level occurs at the physical layer. Because of the physical nature of acoustic propagation, the performance of the *same* MAC and routing protocols will be *different* for different frequency allocations. This fact points to the existence of optimal center frequency and system bandwidth for a given set of network protocols.

In this work, this issue is analyzed for a network operating under distance-aware collision avoidance protocol (DACAP) [6] and focused beam routing (FBR) [7]. Rather than simply advocating for this set of protocols, our main contribution is to demonstrate the benefits of properly choosing center frequency, bandwidth, and transmission power according to the network conditions, always keeping an eye on realistic practical implementations of the system.

This paper is organized as follows. In Section II, an overview of the related work is presented. The underwater acoustic channel is reviewed in Section III. The effects resulting from different power and frequency allocation patterns are discussed in Section IV. Discrete power control is reviewed in Section V. Section VI gives a brief summary of DACAP, while in Section VII, the chosen routing technique and the way in which power control is performed are described. Finally, simulation results are discussed in Section VIII, and the paper is concluded in Section IX.

## II. RELATED WORK

Underwater acoustic networks have recently attracted a lot of interest in the research community. While some of the existing solutions in the radio-domain may be reused, the unique properties of the underwater channel usually require the development of dedicated solutions. Extensive work at the different layers of the classical protocol stack has been conducted up to date. A good overview of existing networking protocols for underwater networks can be found in [8]. In this section, we focus on the work related to multihopping analysis, power control, and routing.

From an information theoretic point of view, the concept of multihopping and its benefits in the underwater acoustic channel have been recently addressed in the literature. In [9], the capacity of an acoustic relay link is analyzed for a noise-limited scenario, showing that it increases with the number of hops used to span a given distance. This serves as an upper bound for all practical systems in which the channel access must be regulated, in either a deterministic or a random fashion. The capacity of a system based on deterministic access was addressed in [10], while the capacity of a system based on random access was addressed in [11]. Similarly, in [12], a single 1-D relay link is ana-

lyzed and numerically assessed in light of the characteristics of the underwater channel.

The benefits of multihopping are available only if nodes can efficiently adapt their transmission power to the network conditions. While power control for radio wireless networks has been widely addressed in the literature [13]–[16], the number of solutions for the underwater systems is still very limited. In [17], discrete power control for underwater acoustic networks is introduced, and the system performance is evaluated for different scenarios and frequency allocation patterns. When using discrete power control, nodes select the transmission power from a finite set of power levels. It is important to note that while power control can easily be implemented in radio-frequency (RF) transceivers, the number of currently available acoustic transceivers with power control capabilities is certainly limited.

When it comes to routing, techniques based on location information, i.e., geographical routing techniques, seem suitable for the underwater domain, where bottom-mounted nodes have knowledge of their location upon deployment, and mobile nodes (such as AUVs) have local navigation systems. Without location information, a large number of broadcast or multicast queries may cause unnecessary network flooding, thus reducing the user-perceived throughput and increasing the total energy consumption. This is one of the main limitations in nongeographical *ad hoc* routing protocols. In proactive protocols (e.g., destination-sequenced distance vector routing protocol (DSDV) [18], optimized link state routing protocol (OLSR) [19]), or reactive protocols (e.g., *ad hoc* on-demand distance vector routing protocol (AODV) [20], dynamic source routing (DSR) [21]), and their different variations, large signaling overhead and high latency may compromise the network performance.

There are several routing protocols based on location information, which are explicitly designed for the underwater channel. In [22], the authors propose a vector-based forwarding protocol for sensor networks, in which a virtual transmission pipe is defined at each hop of the transmission path. In [23], the design of minimum energy routes is assessed, showing that in dense networks there is an optimal number of hops beyond which the system performance does not improve. In [24], two distributed routing algorithms are introduced for delay-insensitive and delay-sensitive applications. In [7], a novel geographical routing methodology for underwater acoustic networks is proposed and coupled with power control. This technique, called the FBR, is shown to be able to dynamically establish routes on demand without compromising the overall network performance.

While conventional modular design of networks can ease the task of performance evaluation and implementation, only the combination of the functionalities of different layers can achieve optimal performance. In [25], the authors propose a multipath routing protocol based on continuous power control aimed at providing reliable data transfer for time-critical applications in underwater acoustic networks. While providing a major contribution in terms of data reliability and error recovery analysis, relevant issues such as energy consumption during reception of a packet, or when idling, are not considered in this analysis. These are usually negligible, but if power and frequency are properly allocated as functions of the distance, the energy

consumed for reception and idle listening can no longer be neglected. In [26], a mathematical framework for cross-layer optimization is set, and a protocol based on this framework is presented. The proposed solution reflects the different interlayer relations and the unique properties of the channel. Based on the knowledge of the distance between a transmitter and its next relay, the optimal communication parameters in terms of power, frequency, bandwidth, and error-correction techniques are established, and conveyed to the next receiver using a common channel. However, the lack of an acoustic transceiver that is able to dynamically adjust to the instantaneous link conditions limits the usefulness of this approach in practice.

Different from the contributions described in this section, in this paper, we present a cross-layer solution for underwater acoustic networks, and evaluate its performance in terms of energy consumption, end-to-end delay, and number of collisions, for different power and bandwidth allocation schemes, with an eye towards practical implementation. We believe that the proposed cross-layer design is able to efficiently exploit the opportunities of the underwater channel while still remaining practical enough for real implementation.

### III. REVIEW OF THE UNDERWATER CHANNEL

#### A. Attenuation

Attenuation, or path loss that occurs in an underwater acoustic channel over a distance  $l$  in meters for a tone of frequency  $f$  in kilohertz is given in decibels by

$$10 \log_{10} (A(l, f)/A_0) = k10 \log_{10} l + \frac{l}{10^3} 10 \log_{10} a(f) \quad (1)$$

where  $A_0$  is a normalizing constant,  $k$  denotes the spreading factor, and  $a(f)$  is the absorption coefficient. This last parameter is expressed empirically using Thorp's formula in decibels per kilometer for  $f$  in kilohertz as [27, pp. 10–11]

$$10 \log_{10} a(f) = 0.11 \frac{f^2}{1 + f^2} + 44 \frac{f^2}{4100 + f^2} + 2.75 \times 10^{-4} f^2 + 0.003. \quad (2)$$

This formula is generally valid for frequencies above a few hundred hertz, our range of interest. The absorption coefficient increases rapidly with frequency, thus imposing a limit on the maximal usable frequency for an acoustic link of a given distance.

#### B. Noise

The ambient noise in the ocean can be modeled using four different sources: turbulence, shipping, waves, and thermal noise. In our range of interest, the overall power spectral density (p.s.d.) of the noise in dB re  $1 \mu\text{Pa}^2/\text{Hz}$  (i.e., the power per unit bandwidth associated with the reference sound pressure level of  $1 \mu\text{Pa}$ )<sup>1</sup> can be approximated as

$$10 \log_{10} N(f) = \eta_0 - 18 \log_{10} f \quad (3)$$

<sup>1</sup>An acoustic signal propagates as a pressure wave whose level is commonly measured in decibels relative to 1 micro-Pascal. In seawater, 1 W of acoustic power radiated from a point source will create a sound field of 170.8 dB re  $1 \mu\text{Pa}$  over the surface of a 1-m radius sphere centered at the source [28, pp. 130–133].

where  $f$  is in kilohertz, and the constant level  $\eta_0$  is adjusted in accordance with a specific deployment site. For example,  $\eta_0$  is taken to be 50 dB re  $1 \mu\text{Pa}^2/\text{Hz}$  for the quiet deep sea. The overall p.s.d. of noise decays with frequency, thus limiting the useful acoustic bandwidth from below.

#### C. Propagation Delay

The nominal speed of sound in the water is 1500 m/s, which is 200 000 times lower than the speed of electromagnetic waves in the air. This causes long propagation delays in underwater acoustic systems. While the delay between two nodes in wireless radio networks is on the order of several microseconds, which is usually negligible with respect to a typical packet duration, in underwater acoustic networks, it can reach several seconds for each hop through the network. This delay is comparable or even greater than the typical packet transmission time, making existing networking protocols ill-suited in most cases.

## IV. RESOURCE ALLOCATION

In contrast to the radio-frequency spectrum, the acoustic spectrum is not regulated (yet). However, taking into account the bandwidth limitations caused by the acoustic path loss and the ambient noise, the frequency allocation possibilities are not very numerous.

In this section, we discuss the relationship between transmission distance, power, and bandwidth and introduce the frequency allocation methodology that we will use throughout the paper.

#### A. The AN Product and the SNR

The narrowband signal-to-noise ratio (SNR), which is a dimensionless measure, is given by [5]

$$\text{SNR}(l, f) = \frac{S(f)\Delta f/A(l, f)}{N(f)\Delta f} = \frac{S(f)}{A(l, f)N(f)} \quad (4)$$

where  $S(f)$  is the p.s.d. of the transmitted signal and  $\Delta f$  is a narrow frequency band around  $f$ . The factor  $10 \log_{10} 1/(A(l, f)N(f))$  in dB re  $1 \mu\text{Pa}^2/\text{Hz}$  is illustrated in Fig. 1. For each transmission distance  $l$ , there clearly exists an optimal frequency  $f_o(l)$  for which the narrowband SNR is maximized. Note that this result is invariant to the fixed noise p.s.d. level  $\eta_0$ . In practice, this level can include a margin to guarantee sufficient transmission power to close the link.

#### B. Bandwidth Definition

We define the 3-dB bandwidth below the maximum value of the  $\text{SNR}(l, f)$ ,  $B_{3\text{dB}}(l)$  in hertz, as the range of frequencies around  $f_o(l)$  for which  $A(l, f)N(f) < 2A(l, f_o(l))N(f_o(l))$ . The optimal frequency  $f_o(l)$  and its corresponding  $B_{3\text{dB}}(l)$  as a function of the transmission distance are plotted in Fig. 2. Also shown is the center frequency  $f_c(l)$  of the optimal 3-dB bandwidth, which is different from  $f_o(l)$  because of the asymmetry of the SNR behavior (see Fig. 1). As the transmission distance is reduced, the optimal frequency increases and so does its corresponding 3-dB bandwidth.

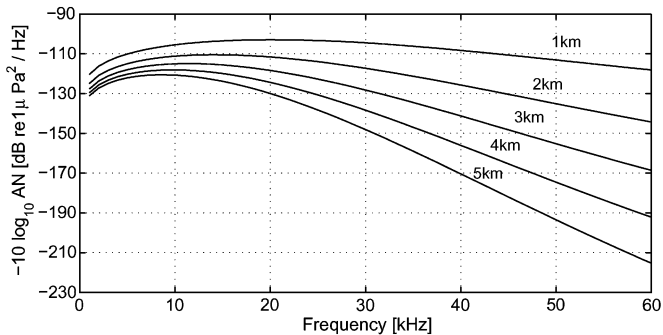


Fig. 1. Frequency-dependent part of the narrowband SNR in decibels,  $10 \log_{10} 1/(A(l, f)N(f))$ , for different transmission distances (attenuation constant  $A_0 = 30$  dB, spreading factor  $k = 1.5$ ).

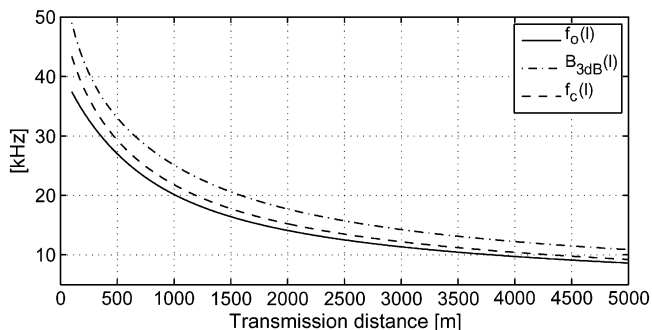


Fig. 2. Optimal frequency  $f_o(l)$ , 3-dB bandwidth  $B_{3\text{dB}}(l)$ , and center frequency  $f_c(l)$  (spreading factor  $k = 1.5$ ).

### C. Transmission Power

Assuming that the transmitted signal p.s.d. is flat across the 3-dB bandwidth, the transmission power in watts necessary to provide a target  $\text{SNR}_0$  at a distance  $l$  in meters from the source is determined as

$$P(l) = \text{SNR}_0 B_{3\text{dB}}(l) \frac{\int_{B_{3\text{dB}}(l)} N(f) df}{\int_{B_{3\text{dB}}(l)} A^{-1}(l, f) df}. \quad (5)$$

We note that this is not the optimal way to shape the spectrum of the transmitted signal; however, it is often used in practice and quite sufficient for the purpose of illustrating the networking concepts.

### D. Interference

When several nodes are sharing the same channel, interference must be taken into account in the system design. The high absorption of the underwater acoustic channel plays a key role in multihop communications.

Since acoustic absorption increases with frequency, a higher transmission power is needed to cover the same link distances if a higher center frequency is used; see (6). However, at the same time, interference suffers a greater attenuation. Therefore, the number of received packets that are discarded due to interference is expected to decrease, and, consequently, the energy lost in retransmissions is reduced. In [10], it is illustrated how the capacity of a cellular system is also heavily influenced by the choice of the frequency region to which the bandwidth is allocated.

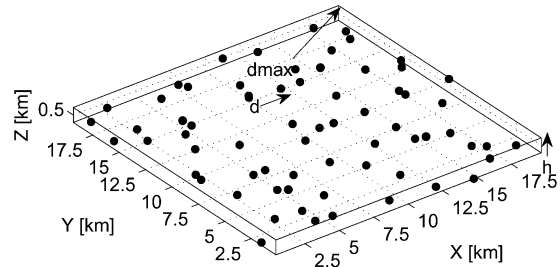


Fig. 3. Simulation scenario: nodes are randomly moving within a 3-D grid.

At a higher center frequency, the available bandwidth is greater, implying greater bit rates. As a result, the total energy consumption is reduced not only because the transmission time is shorter, but also because shorter packets are less likely to collide.

In Section VIII, we will evaluate the effect of changing bandwidth and frequency on the system performance in a network in which MAC and routing functionalities are tightly coupled by the use of power control.

## V. POWER CONTROL

We look at an underwater acoustic network containing both static and mobile nodes as illustrated in Fig. 3. The nodes are able to select their transmission power  $P$  from a finite set of levels  $P_0, P_1, \dots, P_{N-1}$ .

### A. Network Topology and Maximal Transmission Power

We define the maximal transmission power as the smallest amount of power that still guarantees connectivity between any two nodes in the network. Two nodes are said to be physically connected if they can reach each other with a target  $\text{SNR}_0$ . In light of multihop communications, two nodes are connected if there exists at least one path of physically connected nodes between them.<sup>2</sup>

Fig. 3 illustrates the scenario that is being considered. The volume over which the network is deployed is divided using a virtual grid on the  $X - Y$  plane, so that each grid cell contains a node which can move randomly in all three dimensions. In our analysis, we consider that the water depth is much lower than the average node separation in the  $X - Y$  plane. Our focus is on networks with uniformly distributed nodes, whose density is given by

$$\rho = \frac{K}{V} = \frac{1}{d^2 h} \quad (6)$$

where  $V$  is the volume occupied by the network,  $K$  is the total number of nodes in it,  $d$  is the grid-cell side length, and  $h$  is the maximal difference in height between any two nodes. Assuming that the nodes do not move outside their grid cells, the maximal power  $P_{N-1}$  is associated with a transmission distance

$$d_{\max} = \sqrt{5d^2 + h^2}. \quad (7)$$

<sup>2</sup>Due to multipath fading, node failure, and other unpredictable situations, it is not possible to guarantee connectivity between any two nodes at all times, but, on average, this condition will be satisfied with a certain probability.

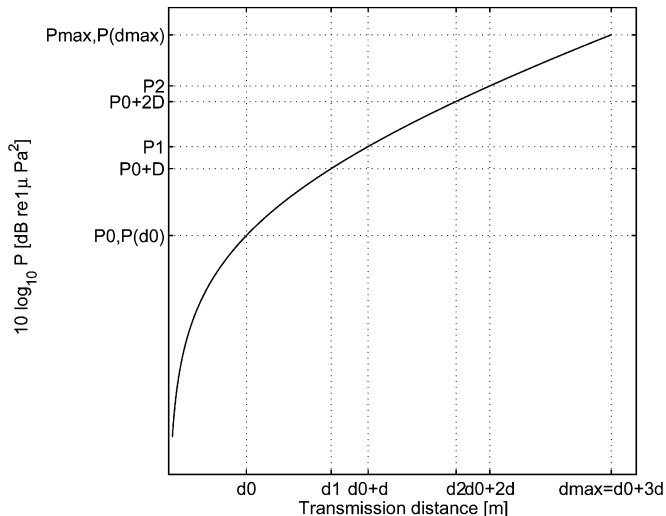


Fig. 4. Power levels and corresponding distances for the two strategies (9) and (10) using a step size  $10 \log_{10} \Delta = 7.2$  dB and  $\delta = 1.56$  km, respectively. The network has 64 nodes deployed over  $400 \text{ km}^2$  in a grid-uniform manner (grid-cell size of  $2.5 \text{ km}$ );  $d_0 = 1 \text{ km}$ ,  $d_{\max} = 5.68 \text{ km}$ ,  $f_c(d) = 14 \text{ kHz}$ ,  $B_{3 \text{ dB}}(d) = 15 \text{ kHz}$ ,  $\eta_0 = 50 \text{ dB re } 1 \mu\text{Pa}^2/\text{Hz}$ ,  $A_0 = 30 \text{ dB}$ ,  $k = 1.5$ ,  $\text{SNR}_0 = 20 \text{ dB}$ .

If this topology is violated, i.e., two nodes become separated by more than  $d_{\max}$ , some parts of the network may lose connectivity. However, in a network that contains mobile nodes, this situation may be only temporary.

### B. Step Size Between Power Levels

Assuming a uniform separation of power levels in decibels, the step size  $10 \log_{10} \Delta$  between two consecutive levels is defined by

$$10 \log_{10} \Delta = (10 \log_{10} P(d_{\max}) - 10 \log_{10} P(d_0)) / (N - 1) \quad (8)$$

with

$$P_n = \Delta^n P_0 = P(d_n), \quad n = 0, \dots, N - 1 \quad (9)$$

where  $d_n$  is the distance in meters corresponding to the power  $P_n$ , i.e., the two are related by the expression (5) and  $d_{N-1} = d_{\max}$ .

Alternatively, the separation between two consecutive levels can be defined in terms of a uniform increase in the coverage distance  $\delta$

$$P_n = P(d_0 + n\delta), \quad n = 0, \dots, N - 1. \quad (10)$$

The incremental distance is obtained as

$$\delta = (d_{\max} - d_0) / (N - 1) \quad (11)$$

and  $d_0 + (N - 1)\delta = d_{\max}$ .

Fig. 4 shows the two power distribution patterns obtained with  $N = 4$  levels, in a network with  $K = 64$  nodes deployed over  $400 \text{ km}^2$ . In this example, the differences between the two power allocation patterns are small, i.e.,  $P(d_n) \approx P(d_0 + n\delta)$ . Due to the convenience of defining the power levels in terms of a

uniform increase in distance, we will use this definition in what follows.

### C. Number of Power Levels

Given a maximal power  $P_{\max} = P(d_{\max})$  and a choice of levels distribution, the last parameter required to completely characterize the power control is the number of levels  $N$ . A greater number of levels allows for finer tuning of the power; however, a smaller number of levels is of interest for practical implementation. We conjecture that there is an effect of diminishing returns in energy savings when it comes to increasing the number of levels beyond some point. The number of power levels will affect the routing protocol performance, as will become apparent in Section VII. We will assess this issue through numerical simulation in Section VIII.

### D. Listening and Receiving Power Consumption

By increasing the node density, the average transmission power required by a node to maintain its connectivity within the network is reduced. However, neither the receiving power nor the listening power depends on the node density, but both are instead implementation-specific modem parameters. These values have usually been considered negligible with respect to the acoustic power needed to cover several kilometers, something that can no longer be assumed in a multihop network.

By using the frequency allocation pattern described in Section IV, the electrical power in decibel watts needed to cover a distance  $l$  is obtained as

$$10 \log_{10} P_T(l) = 10 \log_{10} P(l) - 170.8 - 10 \log \xi \quad (12)$$

where  $10 \log_{10} P(l)$  is the acoustic transmission power in dB re  $1 \mu\text{Pa}^2$ ,  $170.8 \text{ dB}$  is the conversion factor between acoustic pressure in dB re  $1 \mu\text{Pa}$  and acoustic power in watts, and  $\xi$  is the transducer efficiency.<sup>3</sup>

As an example, we can calculate the acoustic power required to provide a target  $\text{SNR}_0$  of  $20 \text{ dB}$  at  $2 \text{ km}$  from the source in quiet deep sea ( $A_0 = 30 \text{ dB}$ ,  $k = 1.5$ ,  $\eta_0 = 50 \text{ dB re } 1 \mu\text{Pa}^2/\text{Hz}$ ). First, the optimal center frequency at  $2 \text{ km}$  is obtained by computing the maximum of (4) with respect to  $f$ , which in this case yields approximately  $14 \text{ kHz}$ . The corresponding 3-dB bandwidth is  $17.72 \text{ kHz}$ . Using these values in the expression (5), the power is found to be  $168 \text{ dB re } 1 \mu\text{Pa}^2$ . For a specific efficiency  $\xi$  equal to  $80\%$ , the equivalent electrical transmission power is approximately  $650 \text{ mW}$ . Note that, in addition to this power, it is necessary to take into account the energy consumed by the power amplifier, the signal processing blocks, and other circuitry of the acoustic modem. Moreover, the energy consumption of these blocks is expected to be higher when the modem is operating at higher frequencies. The power required for listening to the channel varies from modem to modem, ranging from  $500 \mu\text{W}$  [29] to  $80 \text{ mW}$  [30]. Finally, the active reception power can be as low as  $80 \text{ mW}$  or up to a few watts depending on the modem used. The effect of different power specifications on the system energy consumption will be analyzed through simulation in Section VIII.

<sup>3</sup>The transducer efficiency  $\xi$  is usually nonlinear and frequency dependent.

## VI. MEDIUM ACCESS CONTROL

The MAC protocol that is being considered is the DACAP [6], a collision avoidance protocol based on virtual carrier sensing. DACAP implements an exchange of short control packets for avoiding data packet collisions, thus maximizing the network throughput. In addition, it does not require nodes to be synchronous. Hence, it is ideally suited for supporting FBR, which is also based on short control packets exchange, as we will explain in Section VII.

The protocol is based on the following steps.

- Upon receiving a request to send (RTS), a node sends a clear to send (CTS), and waits for a data packet. If during the waiting time another RTS is overheard, the node sends a short warning to its partner.
- Upon receiving a CTS, the transmitter waits for those nodes whose attempts to transmit may result in collisions. If during this time another CTS is overheard or a warning packet arrives, the transmission is deferred by a random backoff time. Otherwise, the transmission of the data packet proceeds.

The waiting time is a function of the round-trip delay, which is proportional to the distance between the nodes. This distance can be easily estimated in FBR, since the responding nodes send their location information. DACAP capitalizes on the receiver's tolerance to interference when the transmitter and the receiver are closer than the transmission range corresponding to the power level used. It does so by computing the minimum distance at which a transmitting node would not interfere with the current transmission, and setting the waiting time accordingly. DACAP was shown to improve the system performance in terms of energy per bit consumption and to successfully account for the hidden terminal problem, at the expense of increasing the average end-to-end delay due to postponements [6].

## VII. ROUTING

The routing technique that is being considered is FBR [7], a routing mechanism based on location information and designed for energy-efficient multihop communications in underwater acoustic networks. This routing mechanism assumes that nodes know their own location and the location of the final destination (sink). Such assumption is justified in underwater systems where fixed bottom-mounted nodes have location information upon deployment, while the mobile nodes, i.e., AUVs, are equipped with internal navigation systems. The location of the final destination is always known in an underwater network in which the distributed nodes are required to transmit to a common sink, or a set of sinks.

### A. Overview of the FBR Protocol

To illustrate the routing protocol, a simple 2-D scenario can be envisioned without loss of generality. Referring to Fig. 5, let us assume that node A wants to transmit to node B. To do so, node A will issue an RTS to its neighbors. This request is a short control packet that contains the location of the source

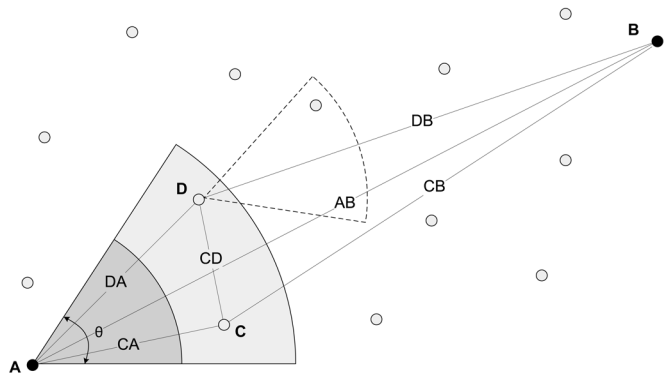


Fig. 5. Illustration of the routing protocol: nodes within the transmitter's cone  $\theta$  are candidate relays.

node (A) and of the final destination (B). Note that this is in fact a multicast request.

The initial transaction is performed at the lowest power level  $P_0$ , and the power is increased only if necessary. Power control is performed as an integral part of routing and MAC. We assume open-loop power control, in which the transmitting node decides which power level to use, rather than being instructed explicitly by a receiving node. Only the nodes that are within the transmission distance are assumed to correctly receive the request.

Returning to our example, let us draw an imaginary line between nodes A and B. All the nodes that receive A's multicast RTS first calculate their location relative to the AB line. The objective in doing so is to determine whether they are candidates for relaying. Candidate nodes are those that lie within a cone of angle  $\pm\theta/2$  emanating from the transmitter towards the final destination. If a node determines that it is within the transmitter's cone, it will respond to the RTS. Those nodes that are outside the cone will not respond.

In our example, there are no nodes within the transmission cone that can be reached at the power level  $P_0$ . Hence, after a round-trip time ( $2d_0/c$  for the power  $P_0$ , where  $c$  is the nominal speed of sound underwater), node A receives no responses. It now increases the transmission power to  $P_1$ , and sends a new RTS. In general, a transmitting node will keep increasing the power until it reaches someone, or until all power levels have been exhausted. If it cannot reach anyone at the maximal level  $P_{N-1}$ , the transmitter will shift its cone and start looking for candidate relays left and right of the main cone. This strategy favors paths with minimal amount of zigzagging, while guaranteeing that all possible paths will eventually be searched. In [23], it was shown that, especially in very dense networks, paths following minimum power routes (maximum number of hops) are not optimal in terms of energy consumption, but that instead there is a minimum distance that should be traversed in each hop (as emphasized in Section V-D). However, the authors also show that for the node densities that we are considering, both options are similar. For this reason, we use these minimum power routes as the gold standard. Alternatively, in very dense networks, this problem could be managed by choosing the initial power level according to the analysis in [23] instead of the lowest available one.

If the transmitter, after increasing the power to some level, reaches a single neighbor, it passes the data packet on to that neighbor, who becomes a relay. A positive acknowledgement at each hop is expected. The relay now initiates an identical procedure, looking for candidate nodes within its own cone. It has become an effective transmitter, searching for the next relay towards the final destination. If there is more than one candidate relay, the current sender will have to decide which one will become the next relay. In our example, A reaches two candidates C and D at power  $P_1$ . (The protocol does not change if there are more than two candidates.) When they receive the RTS from A, each one knows that it can help in relaying, and each replies to A's request using a very short control packet, akin to the clear to send (CTS) signal. A candidate's CTS contains the address (name and location) of the node issuing it (C or D) as well as the addresses of the source and destination (A and B). The two candidate relays are not (yet) aware of each other's existence, so it is possible that their replies will collide. However, because the CTS is very short, and the distances CA and DA are unlikely to be exactly the same, the chances of the two CTS packets colliding at A are minimal. For example, with 500 b in a CTS packet, and a bit rate of 5 kb/s, there will be no collision if the distances CA and DA differ by more than 75 m. Taking into account realistic implementations of acoustic underwater networks, the distance between two nodes will be usually much larger, reducing the probability of collision between candidates. Transmission times may also be randomized to avoid node synchronization effects.

If there is no collision, A receives both replies. A reply includes the sender's location, and, hence, A knows which candidate is closer to the final destination—node D in this case. It may then choose D as the relay, and pass the data packet on to it. Node C will overhear the data packet transaction and deduce from its header that it has not been chosen as a relay. Alternatively, more intelligence can be incorporated into making this decision. For example, A could know from overhearing previous transactions that D is already engaged elsewhere and is thus becoming a bottleneck; it could therefore choose C as its relay. Alternatively, the CTS packet can include information about the network activity that each of the candidates is measuring. In that case, routing is performed by exploiting first- and second-order neighborhood information for more efficient, integrated MAC/routing schemes [31]. This information can be used as part of the relays' decision on whether and when to respond to a multicast RTS. However, such details are of no concern for the basic routing principle.

Although the chances of collision are small, a collision may still happen. If A detects a collision (e.g., by detecting signal energy without being able to decode a packet), it will send the RTS again, using the same power level. In this round, however, C and D may know of each other's existence. This can only be guaranteed if they are inside a cone with an aperture less than or equal to  $60^\circ$ . In this case, they have also learned each other's location, and only that node which knows to be closest to the final destination will reply. Hence, the next CTS collision will be avoided. In a more general case, C and D may not be aware of each other either because of the half-duplex operation of acoustic modems, or because the distance CD is greater than

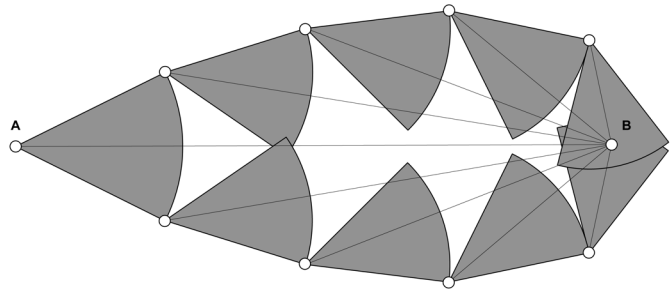


Fig. 6. The region of candidate relay locations is contained within a cone emanating from each relay. The region of all candidate relays which are reachable at the lowest power level is delimited by the shaded beam-like area.

the transmission range associated with the power level in use. In this situation, they will still know that the previous query has not been completed successfully because they will have received exactly the same request as before. Then, they may delay their CTS retransmissions by a random amount  $T_{\text{wait}} = N_{\text{rtx}} T_{\text{CTS}} x$  seconds,<sup>4</sup> where  $N_{\text{rtx}}$  is the number of retransmissions,  $x$  is a random variable uniformly distributed between 0 and 1, and  $T_{\text{CTS}}$  stands for the duration of the reply packet.

When the next relay has been chosen, the procedure continues. The cone emanating from node D is illustrated by dashed lines in Fig. 5. Note that the original sender does not need to know the location of the destination *exactly*. As the route discovery advances, the final relay will reach all the nodes in its own cone, and, so long as the destination has not moved outside this region, it will be reached. Hence, there is a region over which a node can move without affecting the protocol performance. Normally, underwater nodes can be moving at a much slower rate than the speed of propagation (few meters per second as compared to few kilometers per second) and, hence, it is reasonable to assume that a node will not “escape” before it is reached.

As the algorithm progresses, and a cone is formed at each relay, the route will zoom in on the final destination so long as there are candidate relays within reach of one another. Fig. 6 illustrates the region of candidate relay locations for the case when a relay can be found in each hop within a single cone, i.e., no node needs to shift its cone and look outside the angle  $\theta$ . Note that this region is bounded, as dictated by the definition of the transmitter's beam-like cone (hence the name, FBR).

### B. Mobility Issues in the FBR Protocol

Due to drifting, the location of each node may change in time, and, hence, it may not be realistic to assume that each node always knows its own position accurately. If such unintentional motion is caused by a current or an error in navigation, the relative position of the nodes may be preserved at least approximately, in which case the protocol performance will not be significantly affected. At any rate, some power margin can be included in a practical system to account for the possibility of a change in maximal distance. The transmission power used will

<sup>4</sup>It was observed via simulation that by computing the backoff time in this way, the average end-to-end delay was lower than when using the more popular exponential backoff, mainly because the chances of collisions among CTS packets were small.

then be slightly higher than the actual power required to cover a specific distance. In addition, taking into account that there is no need to memorize previously discovered neighbors' positions, mobility does not affect the system performance significantly.

### C. Coupling of DACAP With FBR and Power Control

DACAP already requires an exchange of short packets to secure the channel, and its coupling with FBR is thus natural. The main modifications are summarized below.

- *Multicast requests*—When requesting a route, the transmitter sends a multicast RTS. Each control packet contains three {ID, Position} pairs: one for the current transmitter, one for the final destination, and one for the next intermediate node, i.e., the relay. In a multicast RTS, the last field is left empty. Note that the same RTS packet is looking for a route and securing the channel (similarly with the CTS packets, in which nodes offer to become relays simultaneously as they end the channel reservation procedure). A node proposing itself as a relay overwrites the last field with its own ID and position. After sending a multicast RTS, the transmitter will wait twice the maximum propagation delay corresponding to the current transmission power level even if it has already received one or more CTS packets (plus the corresponding additional delay if it is a retransmitted packet).
- *Silence packets*—After a multicast RTS, the requesting node may receive no answers. This will occur if there are no neighbors, or there are, but they are already engaged in another communication. In the latter case, if the transmitter is not aware of the situation, it will decide to increase the transmission power, increasing the chances of disturbing other ongoing transmissions. To prevent this situation, a node aware of a concurrent communication (but not actively participating in it) that overhears a multicast RTS will send a *very short* silence packet to the requesting node. The silence packet is even shorter than a control packet, because only the destination node should be specified. A node receiving a silence packet will defer its transmission. The chances of its interfering with an ongoing communication are minimal.
- *Implicit acknowledgement*—Apart from an end-to-end acknowledgement which may be generated at the transport or the application layer, each intermediate node expects a positive acknowledgement from the current receiver. If nodes use omnidirectional transducers, which is often the case for mobile nodes, the transmitter can deduce that its last data transaction has been successfully completed when it overhears its own packet being transmitted to the next relay. However, this may not always be possible. If the power level used to reach the next node is lower than the one used for the previous transmission, the acknowledgement should be sent explicitly using a higher power level. The same should be done when the packet reaches its final destination. Also, if for any reason a node receives an RTS from the same transmitter for a packet that has been successfully transmitted (each packet has a unique ID), an acknowledgement is explicitly sent, avoiding the long data packet retransmission.

- *Dynamic backoff and waiting times*—The power level that is being used is specified in each control packet. By doing so, any node that overhears an ongoing communication can dynamically adjust its backoff and waiting times.

Up to this point, the proposed cross-layer design has been qualitatively described. However, the unique relation between transmission distance, power, and bandwidth makes the entire system performance dependent on the frequency allocation pattern. In the following section, we quantitatively demonstrate these concepts by simulation.

## VIII. RESULTS

To assess the concepts introduced in this paper, we have used a discrete-event underwater acoustic network simulator implemented in standard Python [32]. The simulation scenario corresponds to the one shown in Fig. 3. The network is composed of a varying number of active nodes, randomly located over a square footprint of 400 km<sup>2</sup> and with a maximum depth of 1 km. All nodes are moving at 0.2 m/s within their grid cell, and they are assumed to know their approximate location. We assume a fixed noise level  $\eta_0 = 50$  dB re 1  $\mu$ Pa<sup>2</sup>/Hz. In terms of the acoustic wave propagation, an attenuation constant  $A_0 = 30$  dB and a spreading loss  $k = 1.5$  are used. The target SNR for physical connectivity is set to 20 dB. There are four sinks, located in the centers of the four subregions into which the operational region is divided. Each node is able to generate new packets, which will be transmitted to the source's closest sink, potentially over multiple hops. Each node is also able to forward information coming from other nodes.

We assume that the amount of information per area is constant, i.e., the number of packets coming from a region is fixed. A Poisson distribution with an average packet generation rate  $\lambda = 0.01$  (packet/min)/km<sup>2</sup> is used. When the node density is increased, the nodes' individual packet generation rate is reduced in such a way that the total number of bits per second transmitted in the network remains the same. Each data packet contains a fixed number of bits, 9600 in our simulation, while the control packets are only 48 b long.

The system performance is measured in terms of average energy per bit consumption.<sup>5</sup> The energy invested in transmission, listening, and active reception of control and data packets, as well as their possible retransmissions, is taken into account, and divided by the total number of useful information bits delivered to the destinations. The power required for listening to the channel and the power required for active reception are set to 0 dBW. In addition to the energy per bit, the total number of collisions and the average packet end-to-end delay are also measured to illustrate the performance.

Before focusing on the effects of different frequency allocation patterns and power specifications, the benefits of using power control are analyzed.

<sup>5</sup>The energy consumption will in general depend on the level of reliability that we want to guarantee in the network. In our study, we assumed a maximum retry limit of four transmissions per hop, which proved to be sufficient to avoid packet dropping in the vast majority of cases, effectively providing full transmission reliability.

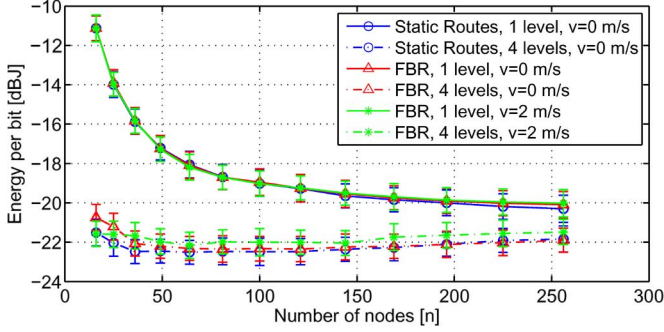


Fig. 7. Energy per bit consumption with and without power control (four uniformly distributed levels). Center frequency and bandwidth are set optimally. The performance of FBR is compared to an ideal case in which node locations are known and Dijkstra’s algorithm is used to compute minimum-power routes. The effect of nodes’ involuntary movements is also illustrated. The error bars represent the uncertainty interval at the 95% confidence level.

### A. Benefits of Power Control

Fig. 7 shows the average energy per bit consumption as a function of the number of nodes. For each node density,  $d_{\max}$  is obtained from (7). The center frequency and the available bandwidth are determined optimally for each node density according to the principles of Section IV, as  $f_c(d)$  and  $B_{3\text{dB}}(d)$ , where  $d$  is the grid-cell side length. The system performance is compared between the case in which a fixed transmission power level covering the distance  $d_{\max}$  is used and when power control with  $N = 4$  levels is available. The FBR performance is compared to that of the case in which routes are established using Dijkstra’s algorithm [33], with the cost between two nodes is defined as the minimal discrete power level required to guarantee connectivity. The SNR required to close the link is set to 20 dB.

As the number of relay nodes increases, the energy consumption reduces mainly because the maximal transmission distance scales with the network density as (7). Therefore, even for a constant transmission power, i.e.,  $N = 1$ , the energy consumption is clearly reduced. This is due not only to the fact that the transmission power is lower for a lower internode distance, but also to the fact that the bandwidth available to shorter links is greater. Hence, a data packet containing the same number of bits takes less time to transmit at a higher bit rate. Note that we are introducing active nodes in the system, i.e., nodes which are generating information and relaying incoming packets, and adapting their packet generation rate in such a way that the amount of information per area remains constant. We can also think of a different situation in which only relay nodes are introduced. The effect on the system energy per bit consumption is almost the same and was discussed in [17].

The benefits of power control are clear, especially for lower node densities, where the minimum transmission distance necessary to maintain the network connectivity is considerably large. The difference between the *distributed* FBR protocol, in which routes are dynamically established as packets traverse the network towards their final destination, and the *centralized* case, in which preestablished routes are followed, is minimal. Note that Dijkstra’s algorithm requires full knowledge of the topology, whereas FBR does not assume any knowledge except for a node’s own location and that of the destination. In

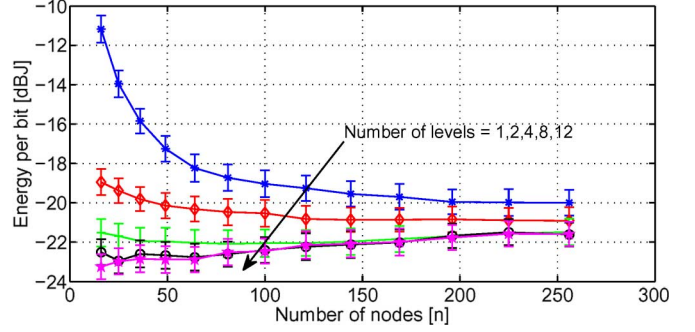


Fig. 8. Energy per bit consumption for a varying number of power levels. Center frequency and bandwidth are chosen optimally; FBR is used. The error bars represent the uncertainty interval at the 95% confidence level.

addition, we can see that nodes’ involuntary movements do not damage the FBR performance and the effect on the energy per bit consumption is minimal. This demonstrates the superiority of the FBR protocol and the fact that exact information is not indispensable.

### B. Number of Power Levels

Using more than one power level allows the system to allocate the power in a more efficient manner. Only those nodes that require the highest transmission power will use it, while all other nodes can use lower levels. By increasing the number of power levels, the power can be adjusted more accurately, reducing the total energy consumption, as well as interference. However, having to use too many power levels may not be practical, and the question remains as to whether there is some number of levels that reaches a good compromise between energy efficiency and implementation complexity. At the same time, increasing the number of available power levels too much can increase the average delay introduced by the route discovery process, which may have to sequentially query several neighbors before finding a relaying node.

Fig. 8 shows the average energy per bit consumption as a function of the number of nodes for a varying number of power levels. It reveals that using more than four levels does not significantly improve the system performance, which supports the conjecture made earlier in Section V. Therefore,  $N = 4$  power levels suffice for the network under consideration, and, for a node density within the range that we illustrate, offer a good compromise between energy per bit consumption and implementation complexity.

### C. Listening and Receiving Power

When the network node density is increased, the power required to successfully transmit a packet is reduced because the maximal transmission distance is shorter. However, the power required by each node for listening or active reception remains the same. Therefore, when the number of nodes in the system increases, the total power required for listening and receiving increases as well. The increase in bandwidth results in a reduced energy consumed for active reception, but the energy required for listening does not change.

This is illustrated in Fig. 9, where the energy per bit consumption as a function of the network node density is shown

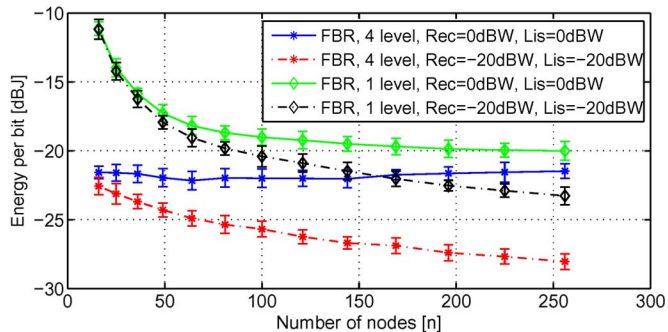


Fig. 9. Energy per bit consumption for different listening and receiving power specifications, with and without power control (four uniformly distributed power levels). The error bars represent the uncertainty interval at the 95% confidence level.

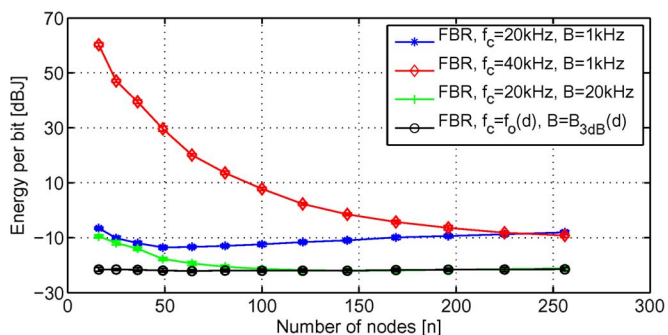


Fig. 10. Energy per bit consumption for different frequency allocation patterns. Power control is implemented with four uniformly distributed power levels. The error bars represent the uncertainty interval at the 95% confidence level.

for different listening and receiving power levels. Two cases are considered, one in which power control with  $N = 4$  power levels is used, and another without power control. The results show the effect of the listening and receiving powers, which has been usually masked by the large acoustic power requirement. These results encourage the development of idle-time energy saving mechanisms such as sleeping cycles or wake up modes in acoustic modems, e.g., [34].

#### D. Frequency Allocation

In the previous sections, both  $f_c$  and  $B_{3dB}$  have been optimized for power consumption according to the channel model used in Section III. Here, we illustrate the effect of independently changing these two parameters while using power control with four uniformly spaced levels. In Figs. 10–12, the energy per bit consumption, the total number of collisions in the network, and the average packet end-to-end delay for four different frequency allocation patterns are shown as functions of the node density. Below we comment on the impact of these design parameters on the network performance.

*Center frequency ( $f_c$ ):* The system performance is analyzed for two different center frequencies  $f_c = 20$  kHz and  $f_c = 40$  kHz, keeping the bandwidth fixed and equal to 1 kHz. As discussed in Section IV, at a higher center frequency, the power consumption for the same internode distance is increased because the acoustic path loss is higher. For this reason, the energy performance is better at 20 kHz than at 40 kHz, but this is only

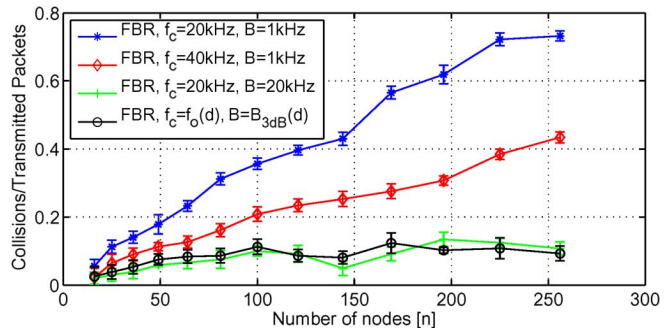


Fig. 11. Total number of collisions over transmitted packets for different frequency allocation patterns. Power control is implemented with four uniformly distributed power levels. The error bars represent the uncertainty interval at the 95% confidence level.

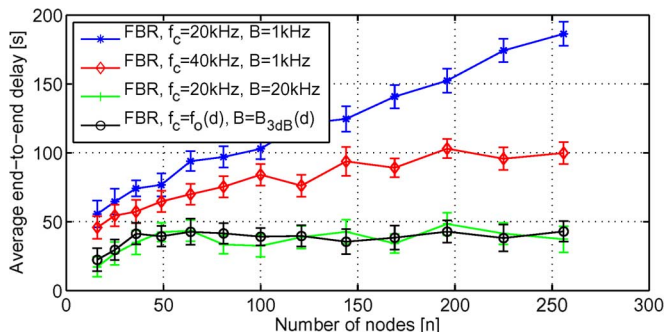


Fig. 12. Average packet end-to-end delay for four different frequency allocation patterns. Power control is implemented with four uniformly distributed power levels. The error bars represent the uncertainty interval at the 95% confidence level.

so for lower densities. In denser networks, where the transmission distance is small, the energy per bit consumption is nearly the same (Fig. 10).

As the center frequency increases, the interference coming from other nodes also suffers a greater attenuation. Therefore, the total number of collisions in the system can be reduced by increasing the center frequency. This effect can be more clearly seen at high node densities, for which the number of collisions is usually higher (Fig. 11). Because the transmission power scales with the network density, the total energy lost in collisions is small. At the same time, the end-to-end delay clearly benefits from the reduction in the number of collisions due to a smaller number of retransmissions especially during the discovery process (Fig. 12).

*Bandwidth ( $B$ ):* The system performance is analyzed for two different bandwidths  $B = 1$  kHz and  $B = 20$  kHz, when the center frequency remains fixed and equal to 20 kHz. The energy per bit consumption benefits from a greater bandwidth for two reasons. First, the bit duration  $1/B$  is reduced; thus, the energy per bit reduces (see Fig. 10). Granted, as the bandwidth increases so does the total noise power that affects the system performance; however, when the increase in bandwidth is coupled with a shortening of the transmission range, the overall effect on the total transmitted energy per bit required to maintain a desired SNR is positive [9]. Second, packets are shorter and, therefore, less likely to collide (Fig. 11). This combined effect encourages transmission at high bit rates: even if the application

does not require it, the system performance in terms of energy per bit consumption and average packet end-to-end delay will improve.

*Summary: combined effects  $f_c$  and  $B$ :* When choosing the center frequency and the bandwidth using the minimum power approach introduced in Section IV, both the optimal center frequency and its corresponding 3-dB bandwidth increase with the node density. In other words, the average internode distance is shorter for a higher node density (Fig. 7) and, hence, the optimal frequency and the available bandwidth are higher (Fig. 2). As the bandwidth increases, both energy per bit consumption and end-to-end delay are reduced because packets are shorter and less likely to collide.

The benefits of changing both the center frequency and the bandwidth according to the network node density are illustrated in Figs. 10–12. The energy per bit reaches a floor, which will not be reduced by increasing the number of nodes in the system. When compared to other frequency allocations, we can see that even when using a constant considerably large bandwidth (20 kHz) the system performance in terms of energy per bit consumption can deteriorate, especially in sparse networks, because higher center frequencies should be selected to support this bandwidth.

## IX. CONCLUSION

In this paper, discrete power control has been considered as a practical means for enabling scalable multihop communications for large coverage areas in bandwidth-limited underwater acoustic networks. Different power allocation schemes with a varying number of available power levels have been considered for varying network densities. For a chosen 3-D example scenario, it has been shown that a finite number of uniformly distributed power levels suffice to achieve energy consumption close to minimum. This number of levels is low enough to motivate a practical implementation of power control, which is seen as a major technique for enabling scalable and energy-efficient coverage of large areas.

The effect on the overall system performance of different modem specifications, i.e., the listening and receiving powers, has also been analyzed, emphasizing the need for idle-time energy saving techniques. Introducing new relaying nodes in the network has an implicit energy cost related to their power consumption even while being idle, which leads to a tradeoff between the power saved by shortening the hop length and the power invested in listening.

The main benefits in terms of the system energy consumption can only be achieved when both power and frequency allocation are adjusted in accordance with the network node density. Due to the dependence of the acoustic path loss on both the distance and the frequency, shorter links are able to utilize higher center frequencies, allowing the system to exploit greater bandwidths. The center frequency and bandwidth were shown to have an effect on the proposed set of protocols, and this would be so for any other selection of protocols. For a higher center frequency, the power required to make up for the greater acoustic path loss is higher, but the interference also attenuates more. This effect translates into a reduction of the number of collisions, which in turn reduces the average end-to-end delay.

The principal improvement in performance comes from the increase in the available bandwidth. The total energy consumed decreases not only because the transmission time per bit is shorter, but also because shorter packets are less likely to collide. Therefore, the total energy consumed on retransmissions reduces. At the same time, a reduction in the number of collisions implies shorter end-to-end delay. This fact encourages transmission at a high bit-rate even if the application does not require it, as the network performance in terms of energy consumption and end-to-end delay will clearly benefit from it. While our results refer to a particular set of MAC and routing protocols (DACAP and FBR), the same methodology can be used to optimize the power and frequency allocation for an arbitrary communication scenario.

## REFERENCES

- [1] I. F. Akyildiz, D. Pompili, and T. Melodia, "Underwater acoustic sensor networks: Research challenges," *Ad Hoc Netw. J.*, vol. 3, no. 3, pp. 257–279, Nov. 2005.
- [2] J. H. Cui, J. Kong, M. Gerla, and S. Zhou, "The challenges of building mobile underwater wireless networks for aquatic applications," *IEEE Network*, vol. 20, no. 3, pp. 12–18, May 2006.
- [3] J. Heidemann, W. Ye, J. Wills, A. Syed, and Y. Li, "Research challenges and applications for underwater sensor networking," in *Proc. IEEE Wireless Commun. Netw. Conf.*, Apr. 2006, pp. 228–235.
- [4] U. M. Cella, R. Johnstone, and N. Shuley, "Electromagnetic wave wireless communication in shallow water coastal environment: Theoretical analysis and experimental results," in *Proc. 4th ACM Int. Workshop Underwater Netw.*, Sep. 2009, article no. 9.
- [5] M. Stojanovic, "On the relationship between capacity and distance in an underwater acoustic communication channel," *ACM SIGMOBILE Mobile Comput. Commun. Rev.*, vol. 11, no. 4, pp. 34–43, Oct. 2007.
- [6] B. Peleato and M. Stojanovic, "Distance aware collision avoidance protocol for ad-hoc underwater acoustic sensor networks," *IEEE Commun. Lett.*, vol. 11, no. 12, pp. 1025–1027, Dec. 2007.
- [7] J. M. Jornet, M. Stojanovic, and M. Zorzi, "Focused beam routing protocol for underwater acoustic networks," in *Proc. 3rd ACM Int. Workshop Underwater Netw.*, Sep. 2008, pp. 75–82.
- [8] D. Pompili and I. F. Akyildiz, "Overview of networking protocols for underwater wireless communications," *IEEE Commun. Mag.*, vol. 47, no. 1, pp. 97–102, Jan. 2009.
- [9] M. Stojanovic, "Capacity of a relay acoustic channel," in *Proc. IEEE OCEANS Conf.*, Oct. 2007, DOI: 10.1109/OCEANS.2007.4449214.
- [10] M. Stojanovic, "Design and capacity analysis of cellular-type underwater acoustic networks," *IEEE J. Ocean. Eng.*, vol. 33, no. 2, pp. 171–181, Apr. 2008.
- [11] C. Benson, M. Ryan, and M. Frater, "On the benefits of high absorption in practical multi-hop networks," in *Proc. IEEE OCEANS Conf. Eur.*, Jun. 2007, DOI: 10.1109/OCEANSE.2007.4302280.
- [12] W. Zhang, M. Stojanovic, and U. Mitra, "Analysis of a simple multihop underwater acoustic network," in *Proc. 3rd ACM Int. Workshop Underwater Netw.*, Sep. 2008, pp. 3–10.
- [13] J. Gomez and A. Campbell, "Variable-range transmission power control in wireless ad hoc networks," *IEEE Trans. Mobile Comput.*, vol. 6, no. 1, pp. 87–99, Jan. 2007.
- [14] J. Ebert, E. Wiederhold, and A. Wolisz, "An energy-efficient power control approach for WLAN's," *J. Commun. Netw.*, vol. 2, pp. 197–206, 2000.
- [15] M. Kubisch, H. Karl, A. Wolisz, L. Zhong, and J. Rabaey, "Distributed algorithms for transmission power control in wireless sensor networks," in *Proc. IEEE Wireless Commun. Netw. Conf.*, Mar. 2003, vol. 1, pp. 558–563.
- [16] S. Lin, J. Zhang, G. Zhou, L. Gu, J. A. Stankovic, and T. He, "ATPC: Adaptive transmission power control for wireless sensor networks," in *Proc. 4th Int. Conf. Embedded Netw. Sens. Syst.*, 2006, pp. 223–236.
- [17] J. M. Jornet and M. Stojanovic, "Distributed power control for underwater acoustic networks," in *Proc. IEEE OCEANS Conf.*, Sep. 2008, DOI: 10.1109/OCEANS.2008.5151829.
- [18] C. E. Perkins and P. Bhagwat, "Highly dynamic destination-sequenced distance-vector routing (DSDV) for mobile computers," *ACM SIGCOMM Comput. Commun. Rev.*, vol. 24, no. 4, pp. 234–244, 1994.

- [19] P. Jacquet, T. Clausen, A. Laouiti, A. Qayyum, and L. Viennot, "Optimized link state routing protocol for ad hoc networks," in *Proc. IEEE Multi Topic Conf.*, 2001, pp. 62–68.
- [20] C. E. Perkins and E. M. Royer, "Ad-hoc on-demand distance vector routing," in *Proc. IEEE 2nd Workshop Mobile Comput. Syst. Appl.*, Feb. 1999, pp. 90–100.
- [21] D. B. Johnson, D. A. Maltz, and J. Broch, *DSR: The Dynamic Source Routing Protocol for Multihop Wireless Ad Hoc Networks*. Reading, MA: Addison-Wesley, Dec. 2000, ch. 5, pp. 139–172.
- [22] N. Nicolaou, A. See, P. Xie, J. H. Cui, and D. Maggiorini, "Improving the robustness of location-based routing for underwater sensor networks," in *Proc. IEEE OCEANS Conf. Eur.*, Jun. 2007, DOI: 10.1109/OCEANSE.2007.4302470.
- [23] M. Zorzi, P. Casari, N. Baldo, and A. Harris, "Energy-efficient routing schemes for underwater acoustic networks," *IEEE J. Sel. Areas Commun.*, vol. 26, no. 9, pp. 1754–1766, Dec. 2008.
- [24] D. Pompili, T. Melodia, and I. F. Akyildiz, "Routing algorithms for delay-insensitive and delay-sensitive applications in underwater sensor networks," in *Proc. 12th ACM Annu. Int. Conf. Mobile Comput. Netw.*, 2006, pp. 298–309.
- [25] Z. Zhou and J. H. Cui, "Energy efficient multi-path communication for time-critical applications in underwater sensor networks," in *Proc. 9th ACM Int. Symp. Mobile Ad Hoc Netw. Comput.*, May 2008, pp. 221–230.
- [26] D. Pompili and I. F. Akyildiz, "A cross-layer communication solution for multimedia applications in underwater acoustic sensor networks," in *Proc. 5th IEEE Int. Conf. Mobile Ad Hoc Sens. Syst.*, Oct. 2008, pp. 275–284.
- [27] L. M. Brekhovskikh and Y. P. Lysanov, *Fundamentals of Ocean Acoustics*. New York: Springer-Verlag, 1991.
- [28] L. E. Kinsler, A. R. Frey, A. B. Coppens, and J. V. Sanders, *Fundamentals of Acoustics*, 4th ed. New York: Wiley, Dec. 2000 [Online]. Available: <http://www.worldcat.org/isbn/0471847895>
- [29] J. Wills, W. Ye, and J. Heidemann, "Low-power acoustic modem for dense underwater sensor networks," in *Proc. 1st ACM Int. Workshop Underwater Netw.*, Sep. 2006, pp. 79–85.
- [30] L. Freitag, M. Grund, S. Singh, J. Partan, P. Koski, and K. Ball, "The WHOI micro-modem: An acoustic communications and navigation system for multiple platforms," in *Proc. IEEE OCEANS Conf.*, Sep. 2005, vol. 2, pp. 1086–1092.
- [31] M. Rossi and M. Zorzi, "Integrated cost-based MAC and routing techniques for hop count forwarding in wireless sensor networks," *IEEE Trans. Mobile Comput.*, vol. 6, no. 4, pp. 434–448, Apr. 2007.
- [32] J. M. Jornet, "AUVNetSim: A simulator for underwater acoustic networks," Massachusetts Inst. Technol., Cambridge, MA, MIT Sea Grant Tech. Rep., 2008 [Online]. Available: <http://seagrant.mit.edu/media/publications/MITSG-08-4.pdf>
- [33] E. W. Dijkstra, "A note on two problems in connection with graphs," *Numerische Mathematik*, vol. 1, pp. 269–271, 1959.
- [34] A. F. Harris, M. Stojanovic, and M. Zorzi, "Idle-time energy savings through wake-up modes in underwater acoustic networks," *Ad Hoc Netw. J.*, vol. 7, no. 4, pp. 770–777, Jun. 2009.



"la Caixa."

**Josep Miquel Jornet** (S'08) received the Engineering Degree in telecommunication engineering and the M.S. degree in information and communication technologies from the School of Electrical Engineering, Universitat Politècnica de Catalunya (UPC), Barcelona, Spain, in 2008. Currently, he is working towards the Ph.D. degree in electrical and computer engineering at the Broadband Wireless Networking Laboratory, School of Electrical and Computer Engineering, Georgia Institute of Technology, Atlanta, with a fellowship from Obra Social

From September 2007 to December 2008, he was a visiting researcher at the MIT Sea Grant, Massachusetts Institute of Technology, Cambridge. His current research interests are in underwater acoustic networks as well as electromagnetic nanonetworks in the terahertz band.

Mr. Jornet is a student member of the Association for Computing Machinery (ACM).



**Milica Stojanovic** (S'90–M'93–SM'08–F'10) graduated from the University of Belgrade, Belgrade, Serbia, in 1988, and received the M.S. and Ph.D. degrees in electrical engineering from Northeastern University, Boston, MA, in 1991 and 1993.

After a number of years with the Massachusetts Institute of Technology (MIT), Cambridge, where she was a Principal Scientist, she joined the faculty of the Electrical and Computer Engineering Department, Northeastern University, in 2008. She is also a Guest Investigator at the Woods Hole Oceanographic

Institution (WHOI), Woods Hole, MA, and a Visiting Scientist at MIT. Her research interests include digital communications theory, statistical signal processing and wireless networks, and their applications to underwater acoustic communication systems.

Dr. Stojanovic is an Associate Editor for the IEEE JOURNAL OF OCEANIC ENGINEERING and the IEEE TRANSACTIONS ON SIGNAL PROCESSING.



**Michele Zorzi** (S'89–M'95–SM'98–F'07) was born in Venice, Italy, in 1966. He received the Laurea degree and the Ph.D. degree in electrical engineering from the University of Padova, Padova, Italy, in 1990 and 1994, respectively.

During academic year 1992/1993, he was on leave at the University of California, San Diego (UCSD) attending graduate courses and doing research on multiple access in mobile radio networks. In 1993, he joined the faculty of the Dipartimento di Elettronica e Informazione, Politecnico di Milano, Milan, Italy.

After spending three years with the Center for Wireless Communications at UCSD, in 1998, he joined the School of Engineering, University of Ferrara, Ferrara, Italy, and in 2003, he joined the Department of Information Engineering, University of Padova, where he is currently a Professor. His current research interests include performance evaluation in mobile communications systems, random access in mobile radio networks, *ad hoc* and sensor networks, energy constrained communications protocols, and underwater communications and networking.

Dr. Zorzi was the Editor-in-Chief of the IEEE WIRELESS COMMUNICATIONS from 2003 to 2005, and is currently the Editor-in-Chief of the IEEE TRANSACTIONS ON COMMUNICATIONS, and serves on the Editorial Board of the *Wiley Journal of Wireless Communications and Mobile Computing*. He was also Guest Editor for special issues in the IEEE PERSONAL COMMUNICATIONS and the IEEE JOURNAL ON SELECTED AREAS IN COMMUNICATIONS. He is a Member-at-Large of the Board of Governors of the IEEE Communications Society.